

Evaluation of the EPL and GFFT algorithms for direct reconstruction of non-Cartesian k-space data

João Luiz Azevedo de Carvalho

ABSTRACT

The most common strategies for reconstructing MR images acquired on an arbitrary k-space trajectory are the gridding algorithm and the direct Fourier transform (DrFT) method. In gridding, the use of the FFT yields in computational efficiency, but the reconstruction accuracy varies according to the density weighting and the convolution kernel being used. The DrFT method does not require a convolution kernel, but it is very time-consuming. Recently, a few new algorithms have been proposed to accelerate the DrFT, including the generalized fast Fourier transform (GFFT) algorithm and the equal-phase line (EPL) algorithm. In this work, these two algorithms are compared to the gridding and DrFT methods in terms of reconstruction accuracy and computational efficiency. The goal here is not only verify the validity of these methods, but also gain understanding on the problem of non-Cartesian reconstruction by describing and implementing these four algorithms.

INTRODUCTION

In order to reduce the scan-time, many alternatives to the 2DFT acquisition method have been proposed. Such sequences are implemented by sampling k-space in trajectories that often do not allow the acquisition on a Cartesian grid. Trajectories such as the spiral, rosette, ROSE, Liassajou, Norton's and sinusoidal are among the most commonly used ones.

However, one of the prices for the reduction in scan time is increased complexity during the reconstruction phase. When k-space data is sampled on a Cartesian grid, the image can be reconstructed simply by using a 2D-DFT. The FFT algorithm is fast and efficient, thus reconstruction complexity is not a problem. On the other hand, non-Cartesian reconstruction can be very slow, since the FFT can't be directly applied. The most common strategies for reconstructing MR images acquired on an arbitrary k-space trajectory are the gridding algorithm and the direct Fourier transform (DrFT) method.

In the gridding algorithm [1], the raw data is first weighted to compensate for the nonuniform sampling density, then convolved with a convolution kernel and resampled onto a Cartesian grid, and finally transformed into image space using the FFT. The use of the FFT yields in computational efficiency, but the reconstruction accuracy varies according to the density weighting and the convolution kernel being used. This sometimes results in a reconstruction that is not as accurate as it might be expected [2].

In the DrFT method [3] the reconstruction is simply a Fourier summation of the raw data weighted with a density compensation function (DCF). The DrFT method has a few advantages over the gridding approach. Since it does not require a convolution kernel, one source of degradation is excluded. Moreover, the MR image can be

dynamically reconstructed by updating the image every time a new k-space data point is acquired. However, the DrFT is very time-consuming which is a major disadvantage. Recently, a few new algorithms have been proposed to accelerate the DrFT, including the generalized fast Fourier transform (GFFT) algorithm and the equal-phase line (EPL) algorithm.

The GFFT algorithm [4] is a 2D extension of an algorithm for the computation of a 1D fast Fourier transform of nonuniformly-spaced data samples [5]. The gain in computational efficiency is related to the use of a FFT to compute most of the calculations required in the DrFT. However, close inspection of the GFFT reveals it to be equivalent to a gridding method with a Gaussian convolution kernel. Thus, it might be considered as a non DrFT-type reconstruction algorithm.

On the other hand, the EPL algorithm [2] can rapidly perform the DrFT reconstruction by distributing the contribution of a data point to the pixels on the image according to equal-phase lines (EPLs). All pixels on an EPL receive the same contribution from the data point, and only a few of the EPLs are required for all pixels on the image. Thus, the computational time of the DrFT reconstruction is considerably decreased.

Both the GFFT and EPL are very recent developments. In this work, these two algorithms are compared to the gridding and DrFT methods in terms of reconstruction accuracy and computational efficiency. The goal here is not only verify the validity of these methods, but also gain understanding on the problem of non-Cartesian reconstruction by describing and implementing these four algorithms.

THEORY

GRIDDING RECONSTRUCTION

In the gridding method, each k-space data point is convolved with a gridding kernel, and that convolution is evaluated at the adjacent grid points. Thus, the result of the convolution for each data point is sampled and accumulated on the Cartesian grid. When all k-space samples have been processed, the inverse FFT is used to reconstruct the MR image.

In k-space, the gridding process can be expressed by the equation

$$\hat{M}(k_x, k_y) = [(M(k_x, k_y) \cdot S(k_x, k_y)) * C(k_x, k_y)] \times III\left(\frac{k_x}{\Delta k_x}, \frac{k_y}{\Delta k_y}\right) \quad (1)$$

where M is the k-space being sampled, S is the non-Cartesian sampling function, C is the gridding kernel, III is the Cartesian sampling function and \hat{M} is the Cartesian-sampled k-space. After the inverse Fourier transform, this becomes

$$\hat{m}(x, y) = [(m(x, y) * s(x, y)) \cdot c(x, y)] * III\left(\frac{x}{FOV_x}, \frac{y}{FOV_y}\right) \quad (2)$$

The convolution with $s(x,y)$ usually results in sidelobes, which are created due to the pattern of the samples in k-space. The multiplication by $c(x,y)$ causes apodization,

which has the undesirable effect of producing shading in the image (which can be compensated in post-processing), but also has the desirable effect of suppressing the sidelobes. Finally, the Cartesian-sampling causes replication in image domain. Thus, the sidelobes may interfere as aliasing in the reconstructed image. This problem can be avoided or reduced simply by using an oversampled grid. In practice, a 2X grid is commonly used, mostly because of the desire to use the next larger power-of-two FFT. However, by using the FFTW package available from *fftw.org*, computational time and memory requirements can be reduced by using a smaller non-power-of-two oversampling. Though, there are tradeoffs between the size and shape of the gridding kernel, the amount of aliasing that can be tolerated, and reconstruction speed. The nature of these tradeoffs is a current research topic. [1]

Another issue with gridding (and all the other non-Cartesian reconstruction methods approached in this work) is the sample density compensation. Because the sampling spacing is nonuniform, the area of k-space associated with each sample is related to the pattern in which the data points are distributed along k-space. During image reconstruction, the contribution of a raw data sample which is associated to a large k-space area should be stronger than the contribution of a sample associated with a smaller area. If proper density weighting is not applied, then regions of k-space with a large concentration of data samples would have an overestimated contribution to the reconstructed images, as during the gridding process, we would have a large concentration of convolved kernels in that area, in contrast to a small concentration of kernels in a low density region. This can be corrected in two ways: *precompensation* and *postcompensation*.

On precompensation, each raw data sample is multiplied by its associated weight before gridding is applied. On the other hand, postcompensation is done after the gridding process, by multiplying the Cartesian-grid samples by a weighting matrix. This weighting matrix can be easily estimated by gridding a unity data vector. The result of this operation is a matrix that reveals the concentration of non-Cartesian raw data samples on the neighborhood of each Cartesian-grid k-space sample. So, the weighting factor for each Cartesian-grid sample should be the inverse of the concentration in that point. However, this method can be used for postcompensation only, so other approaches should be used for the estimation of the weighting function for precompensation. For simple cases, such as spirals, projection and Lissajou, the density can be computed using simple geometry. For more complex cases, numerical approaches can be used for this estimation [1]. A popular choice is to use the Voronoi area [6], which is the area of the set whose points are closer to the given point than to all other k-space sample points.

DrFT RECONSTRUCTION

The direct Fourier transform (DrFT) method is an analytical approach to the problem of non-Cartesian reconstruction. Each pixel of the reconstructed image is computed as the weighted correlation of the sampled FID signal and the phase modulation function for that pixel [3]. Thus, this method can be expressed as

$$m(x, y) = \sum_{n=0}^{N-1} W_n M_n e^{j2\pi(xu_n + yv_n)} \quad (3)$$

where N is the total number of k-space samples, M_n is the raw data acquired at the point (u_n, v_n) on the non-Cartesian grid in k-space and W_n is the weight of that point. The same weighting function used for gridding precompensation can be used here.

However, the DrFT method has a few advantages over the gridding approach. Since it does not require a convolution kernel, one source of degradation is excluded. Moreover, the MR image can be dynamically reconstructed by updating the image every time a new k-space data point is acquired. On the other hand, there is a major disadvantage associated with the DrFT. The calculation is very time-consuming, as for each image pixel we need to compute and accumulate the contribution of each raw data point.

Recently, a few new algorithms have been proposed to accelerate the DrFT. Two of those are discussed next: the generalized fast Fourier transform (GFFT) algorithm and the equal-phase line (EPL) algorithm.

GFFT ALGORITHM

The generalized fast Fourier transform (GFFT) algorithm [4] is a 2D extension of an algorithm for the computation of a 1D fast Fourier transform of nonuniformly-spaced data samples [5]. For reconstructing $m(x, y)$ as an $L \times L$ pixel image, the 2D GFFT can be expressed by the equation

$$\hat{m}(x_c, y_d) = e^{k(x_c^2 + y_d^2)/4} \sum_{a=-rL/2}^{rL/2-1} \sum_{b=-rL/2}^{rL/2-1} \tau_{ab} e^{j\left(\frac{a}{2}x_c + \frac{b}{2}y_d\right)} \quad (4)$$

where $x_c = 2\pi c/L$, $y_d = 2\pi d/L$, r is an ‘‘oversampling’’ factor and c, d span in the interval $[-L/2, L/2-1]$. This expression may be computed using an $rL \times rL$ ordinary 2D FFT. This will give values of $m(x_c, y_d)$ for c and d outside the interval $[-L/2, L/2-1]$. Since we are trying to reconstruct an $L \times L$ pixel image, these extra values are discarded. The matrix τ is defined as

$$\tau_{ab} = \sum_{\{n, j_1 | \mu_n + j_1 = a\}} \sum_{\{n, j_2 | \lambda_n + j_2 = b\}} W_n M_n P_{j_1 n} Q_{j_2 n} \quad (5)$$

where

$$P_{j_1 n} = \frac{1}{2\sqrt{k\pi}} e^{-[r\omega_x(n) - (\mu_n + j_1)]^2 / 4k} \quad \text{and} \quad Q_{j_2 n} = \frac{1}{2\sqrt{k\pi}} e^{-[r\omega_y(n) - (\lambda_n + j_2)]^2 / 4k} \quad (6)$$

and parameters r, k and q are chosen to meet reconstruction accuracy requirements. The choice of $r = 2$ is sufficient for most practical applications [4], and according to [5] the choice of $q = 10$ and $k = 0.5993$ is somewhat optimal. Index j spans in the interval $[-q/2, q/2]$ and n in $[0, N-1]$, where N is the number of k-space non-Cartesian samples M_n which are associated with their respective weights W_n . K-space coordinates are mapped as $\omega_x(n) = 2\pi u_n$ and $\omega_y(n) = 2\pi v_n$, and $\mu_n = [r \omega_x(n)]$ and $\lambda_n = [r \omega_y(n)]$, where $[a]$ is here defined as the closest integer to a .

The gain in computational efficiency is related to the use of a FFT to compute (4). The GFFT algorithm gives an approximation to the DrFT, and the accuracy of this approximation will be affected by the choice of the parameters r , k and q . However, close inspection of the GFFT reveals it to be equivalent to a gridding method with a Gaussian convolution kernel [4]. The computation of matrix τ can be seen as a Cartesian-grid sampling of the convolution of the weighted k-space samples with a separable Gaussian kernel represented by $P_{jn}Q_{jn}$. The FFT transforms the raw data into image domain and then the complex exponential in equation (4) can be seen as deapodization procedure. Thus, the GFFT can be thought as a gridding method and thus it might not be considered a DrFT-type reconstruction algorithm [2].

EPL ALGORITHM

The equal-phase line (EPL) algorithm [2] is proposed as a more efficient way of computing the DrFT. This algorithm is based on the fact that it is not necessary to value equation (3) for each pixel (x,y) on the image because the values are the same at the pixels having the same phase $2\pi(xu_n+yv_n)$.

If a group of pixels has the same phase, the values of the complex exponential function in (3) at these pixels are also the same. Thus, k-space sample M_n has the same contribution to those pixels and (3) can be valued only once for each group. EPL explores this property in order to increase computational efficiency.

Pixels of the same phase are on a straight line in the image space. This line can be described by $xu_n+yv_n = C$ and is called an equal-phase line (EPL). Since the complex exponent function is 2π periodic, than the set of constants C may be limited to the interval $[0,1)$. This interval will be divided into P subintervals to form P EPLs, which are described by

$$xu_n + yv_n = C_p = p / P, \quad p = 0, 1, 2, \dots, P-1 \quad (7)$$

Thus, according to (3) the contribution of the data point M_n to a pixel on an EPL, C_p , is

$$b_n(p) = W_n M_n e^{j2\pi C_p} \quad (8)$$

Therefore, the EPL algorithm can be implemented as follows:

Step 1: set $m(x,y) = 0$ for all pixels.

Step 2: for a given raw data sample, compute $b_n(p)$ for all P values of p .

Step 3: for a given pixel (x,y) , find C and calculate $p = [CP] \bmod P$;

Step 4: add $b_n(p)$ to $m(x,y)$ and $b_n(P-p)$ to $m(-x,-y)$. Note that $b_n(P) = b_n(0)$. Also, for $x = 0$, $m(x,-y)$ and $m(-x,-y)$ are the same pixel and therefore the contributions should not be added twice.

Step 5: go to step 3 for the next pixel of $x \geq 0$.

Step 6: go to step 2 for the next raw data sample.

The accuracy and computational efficiency of the EPL algorithm vary with the number of EPLs. For the DrFT reconstruction of an $L \times L$ image acquired with N raw

data samples, $N \times L^2$ complex MACs (multiplication and accumulation) are required. With EPL, this number is reduced to only $N \times P$, where typical values of P are on the order of 150 to 200 EPLs for an accurate reconstruction. However, the multiplications, truncations and logical operations required for the implementation of step 3 slow down this algorithm and therefore EPL does not run as fast as gridding or the GFFT. In the light of its inherently parallel structure, the most efficient way to speed up EPL would be the use of a multiprocessor system. [2]

MATERIALS AND METHODS

The algorithms described in the previous sections were implemented in Matlab[®] and the reconstructed images obtained with each algorithm were compared. The raw data used for the tests is a simulation of an acquisition done using 6 spiral interleaved trajectories as illustrated in Fig. 1. A total of 9216 k-space samples were used on each reconstruction.

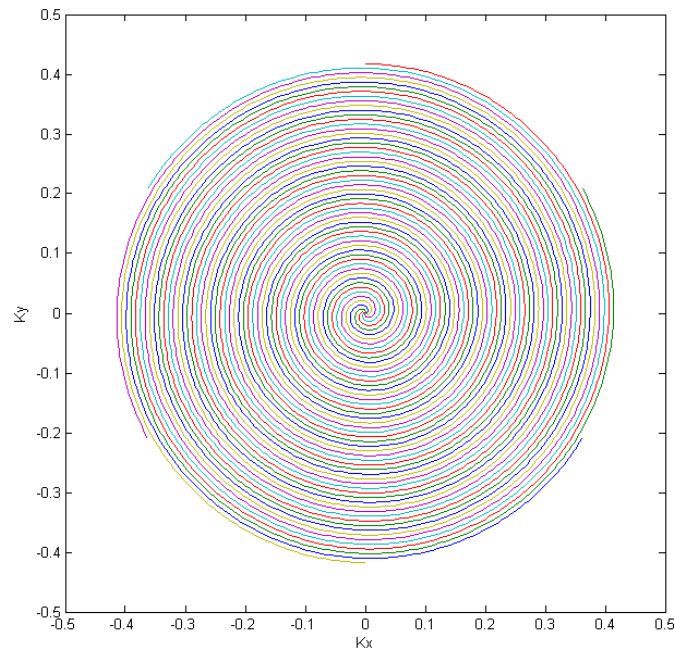


Fig. 1. K-space trajectory used for the reconstructions. Each spiral interleave (presented in different colors) represents a different TR.

The image was reconstructed as 128×128 pixels using all four algorithms. The RMS reconstruction signal-to-error ratio for gridding, GFFT and EPL were computed as

$$SER_{rms} = 20 \log \left(\sqrt{\frac{\sum_x \sum_y (\hat{m}(x, y) - m(x, y))^2}{\sum_x \sum_y m(x, y)^2}} \right) \quad (9)$$

where the DrFT image (Fig. 2) was used as the reference $m(x,y)$. The images were scaled to the same range of gray levels by dividing each pixel of each image by the mean value of that image.

Because the reconstructions were performed in Matlab, the computational efficiency won't be analyzed as a function of processing time, but as the number of complex operations required for the reconstruction process.

For gridding, a 2X Cartesian-grid along with a 2D separable triangular (pyramidal) kernel was used for its simplicity. In practice, a Kaiser-Bessel convolution kernel is being widely used for better reconstruction accuracy [4].

For the GFFT algorithm, the parameters were chosen as $r = 2$, $q = 10$ and $k = 0.5993$, as these values seem to optimize the reconstruction accuracy vs. computational efficiency trade-off [4].

For the EPL algorithm, different numbers of EPLs were used in order to evaluate the trade-off between reconstruction accuracy and computational efficiency.

RESULTS

The reconstructed images as well the respective reconstruction error for each method are shown in Figs. 3-16. The error images have been multiplied by a factor of 8 in order to increase visibility. There is some saturation in the edges of Fig. 4 due to this operation, but it does not affect that other error images at all. The maximum reconstruction error for the GFFT reconstruction was only 0.0041 gray levels (much less than the image quantization precision of 1 gray level) thus the corresponding error image (Fig. 6) is blank.

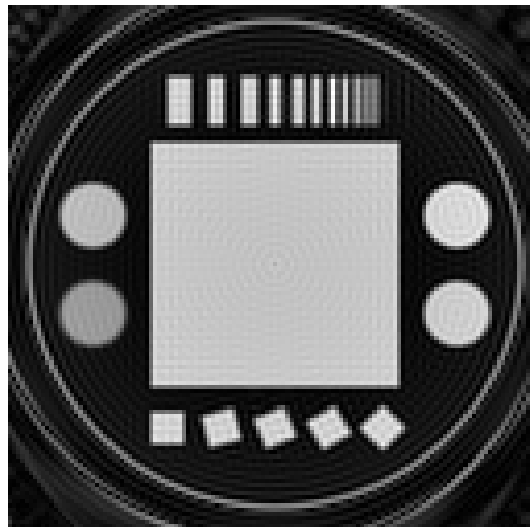


Fig. 2. DrFT reconstructed image (reference)

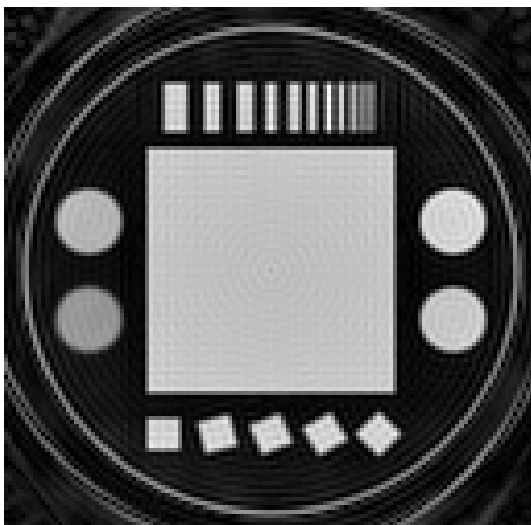


Fig. 3. Gridding reconstructed image

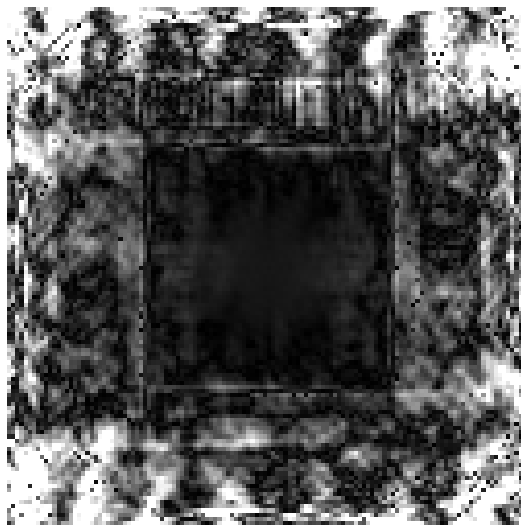


Fig. 4. Gridding reconstruction error (x8)

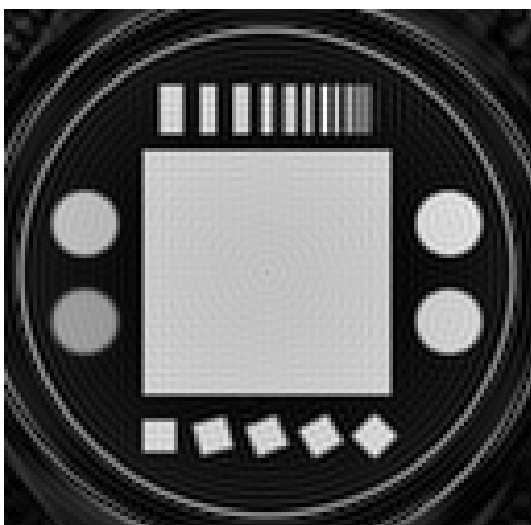


Fig. 5. GFFT reconstructed image

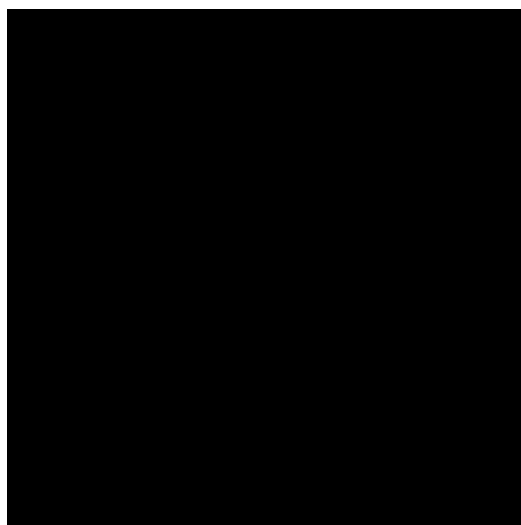


Fig. 6. GFFT reconstruction error (x8)

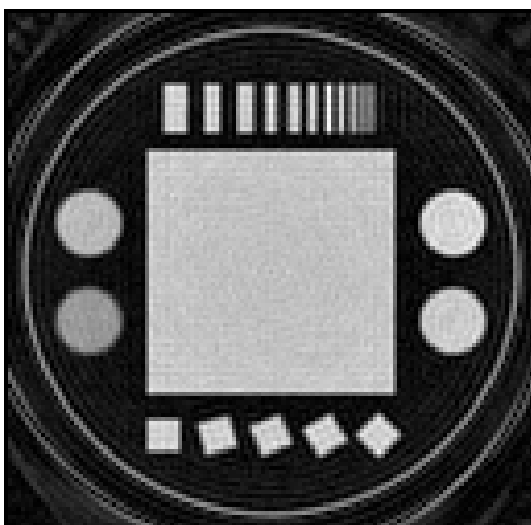


Fig. 7. EPL reconstructed image (P=25)

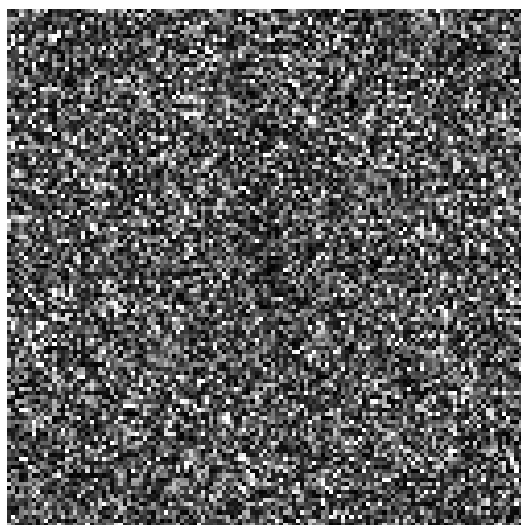


Fig. 8. EPL reconstruction error for P = 25 (x8)

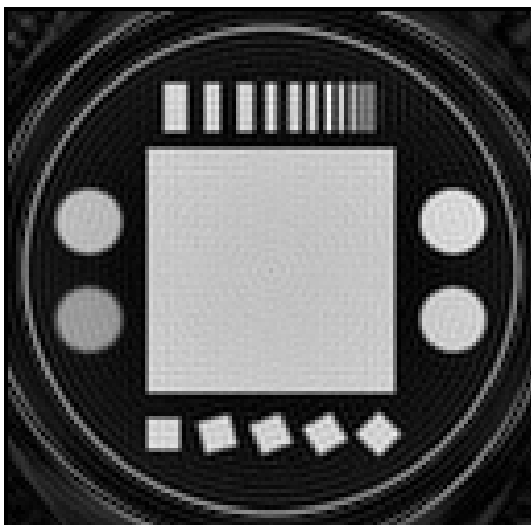


Fig. 9. EPL reconstructed image (P=50)

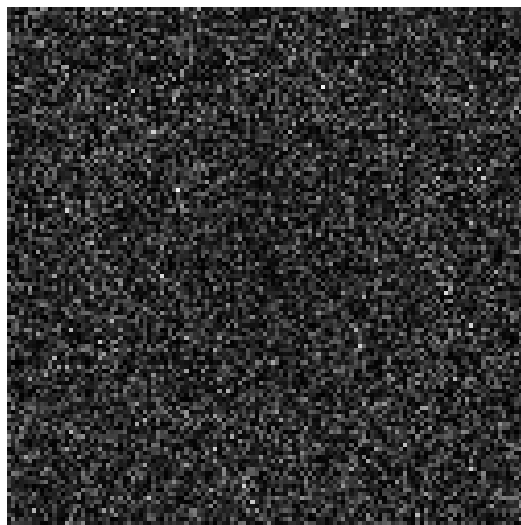


Fig. 10. EPL reconstruction error for P = 50 (x8)

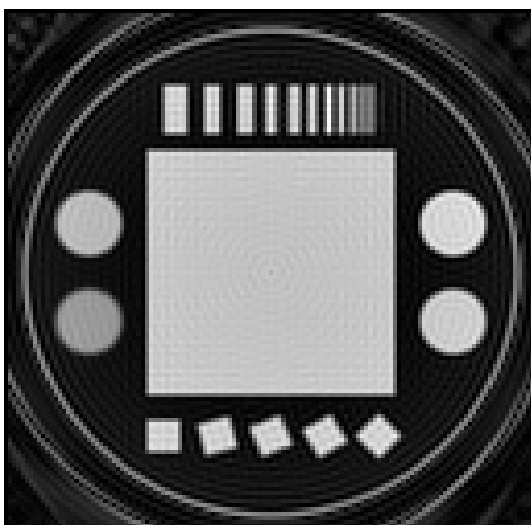


Fig. 11. EPL reconstructed image (P=100)



Fig. 12. EPL reconstruction error for P = 100 (x8)

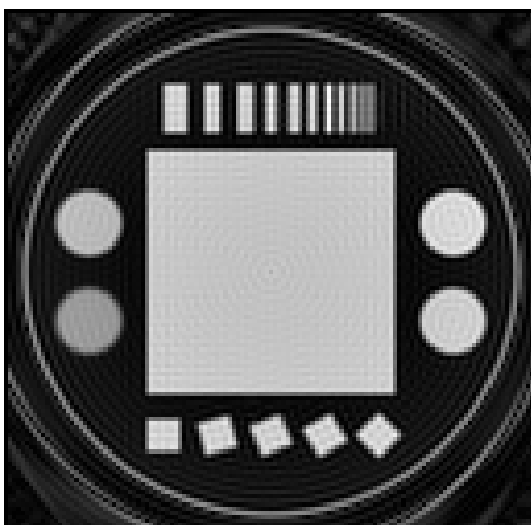


Fig. 13. EPL reconstructed image (P=150)



Fig. 14. EPL reconstruction error for P = 150 (x8)

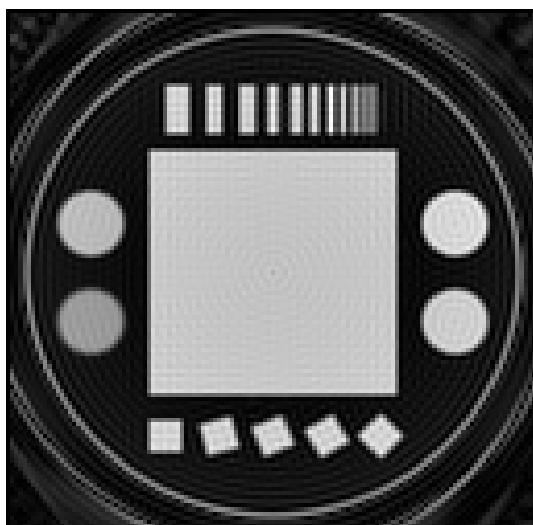


Fig. 15. EPL reconstructed image (P=200) Fig. 16. EPL reconstruction error for P = 200 (x8)

Using equation (9), the reconstruction error was evaluated. The results are presented in Table 1, along with the maximum reconstruction error for each reconstruction. From these results we can plot a curve which presents the reconstruction accuracy as a function of the number of EPLs (Fig. 17).

Table 1 – Signal-to-error ratio (SER) and maximum error for the different reconstructions

Method	SER (in dB)	max. error (in gray levels)
Gridding	27.1	72
GFFT	115.3	0.0041
EPL (P=25)	28.2	64
EPL (P=50)	34.1	31
EPL (P=100)	40.2	14
EPL (P=150)	43.5	10
EPL (P=200)	46.2	7

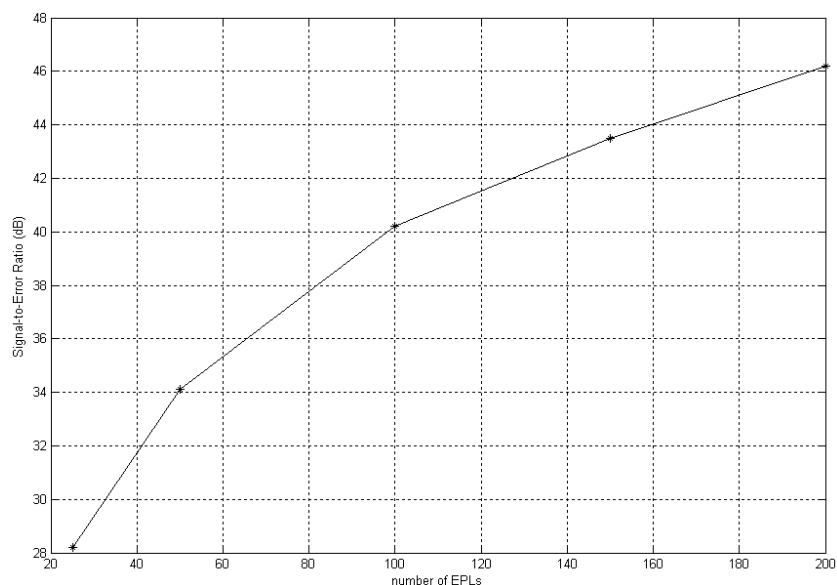


Fig. 17. Signal-to-error as a function of the number of EPLs used for the reconstruction

DISCUSSION

The performance of the gridding algorithm was very poor compared to the other methods in terms of reconstruction accuracy. The reason for this is probably the choice of a very simplistic pyramidal kernel instead of the widely used Kaiser-Bessel kernel. The signal-to-error ratio for gridding was as low as the one obtained using only 25 EPLs for the DrFT approximation. However, with gridding the error is concentrated in the edges of the image, while with EPL the error is spread out and does not show any resemblance with the actual image. Another peculiar observation about the EPL algorithm is that the signal-to-error ratio seems to be increased by of a factor of approximately 6 dB every time the number of EPLs is doubled.

The GFFT algorithm has revealed itself extremely accurate as the reconstruction error is irrelevant when compared to the DrFT reconstruction. However, while there seems to be a large difference of reconstruction accuracy between the GFFT and EPL when evaluating the numerical results, the EPL reconstructed images show that the reconstruction error is quite unnoticeable, even when using as little as 50 EPLs. This is probably due to the fact that the EPL reconstruction error is spread along the whole image and seems to keep no visible relation with the actual image.

In terms of computational efficiency, these methods can be compared by evaluating the number of operations of complex multiplication (OCM) and operations of real multiplication (ORM). In fact, there are four ORMs in one OCM, so we can compute the ORMs as being 1/4 OCM each. Table 2 presents the number of OCMs in the approached methods for a 128^2 image acquired with 9216 raw data points.

Table 2 - Number of operations required for each reconstruction method

Mehtod	Required operations [2] [4]	Total of OCMs ($L = 128$)
Gridding	$N + 36.L^2 + 4.L^2.\log_2(2.L)$	1 M
DrFT	$(3/2).N.(1 + L^2)$	227 M
GFFT ($r = 2, q = 10$)	$[r.L.\log(r.L)+r.L.q]^2$	16 M
EPL ($P = 150$)	$N.[1 + P + (3/8).L^2]$	58 M

Both gridding and GFFT algorithms run very quickly due to the FFT. Actually, GFFT can be made even faster at the cost of reconstruction accuracy, by choosing a smaller q . The operations required in step 3 of EPL slow down this algorithm, and for this reason it is not as fast one might expect, even if a small number of EPLs is used. In fact, the number of EPLs has little weight in the final number of OCMs. Nevertheless, it is still four times faster than DrFT and has the advantage of allowing the image to be updated as each non-Cartesian k-space sample is acquired, while in gridding and GFFT, all raw data samples must be acquired before applying the FFT.

CONCLUSIONS

The performance of the gridding algorithm was very poor compared to the other methods in terms of reconstruction accuracy. The reason for this is probably the choice of a very simplistic pyramidal kernel instead of the widely used Kaiser-Bessel kernel. In EPL the signal-to-error ratio seems to be increased by of a factor of approximately 6 dB every time the number of EPLs is doubled. Since the number of EPLs has little weight on

the computational efficiency, it can be increased in order to improve reconstruction accuracy. The GFFT algorithm has revealed itself extremely accurate as the reconstruction error is irrelevant when compared to the DrFT reconstruction. However, while there seems to be a large difference of reconstruction accuracy between the GFFT and EPL when evaluating the numerical results, EPL reconstructed images show that the reconstruction error is quite unnoticeable, even when using as little as 50 EPLs. This is probably due to the fact that the EPL reconstruction error is spread along the whole image and seems to keep no visible relation to the actual image. Both gridding and GFFT algorithms run very quickly due to the FFT. EPL is slower, but it is still four times faster than DrFT and has the advantage of allowing the image to be updated as each non-Cartesian k-space sample is acquired.

REFERENCES

- [1] Pauly J. Reconstruction of non-Cartesian Data Image. *Reconstruction Textbook*; pp 39-54.
- [2] Qian Y, Lin J, Jin D. Direct reconstruction of MR images from data acquired on a non-Cartesian grid using an equal-phase line algorithm. *Magn Reson Med* 2002;47:1228-1233.
- [3] Maeda A, Sano K, Yokoyama T. Reconstruction by weighted correlation for MRI with time-varying gradients. *IEEE Trans Med Imaging* 1988;7:26-31.
- [4] Sarty GE, Bennet R, Cox RW. Direct reconstruction of non-Cartesian k-space data using a nonuniform fast Fourier transform. *Magn Reson Med* 2001;45:908-915.
- [5] Dutt A, Rokhlin V. Fast Fourier transforms of nonequispaced data. *SIAM J Sci Comput* 1993;14:1368-1383.
- [6] Rasche V, Proska R, Sinkus R, Börner P, Eggers H. Resampling fdata between arbitrary grids using convolution interpolation. *IEEE Trans Med Imaging* 1999;18:385-392